



SEISMIC PERFORMANCE OF LOW STRENGTH CONCRETE COLUMNS WITH CARBON FIBER REINFORCED PLASTIC OF EXISTING BUILDINGS IN JAPAN

Momoyo NEGUCHI¹, Hideo TSUKAGOSHI² and Koichi MINAMI³

ABSTRACT

The seismic diagnosis revealed that there were many buildings of the low strength concrete (LSC) less than 13.5 N/mm^2 . The current seismic diagnosis and retrofit standards have no application in the buildings of LSC and it is essentially to confirm the seismic performance by experiments (The Japan Building Disaster Prevention Association, 2001).

This study reports on the effect of carbon fiber reinforced plastic (CFRP) to LSC by fundamental tests and experimental results of 14 columns with LSC, and propose evaluation method of shear strength by plastic method.

In conclusion, even columns with LSC have the performance as columns and can be retrofitted and shear strength of members with low strength concrete can be calculated by plastic theory. Though the confined effect by CFRP should not be given to the arch mechanism in plastic theory because of the size effect, seismic retrofit by CFRP is recognized as effective against improvement in the shear strength of column with LSC in particular under high axial load or using deformed bars as main reinforcements.

1. INTRODUCTION

Seismic diagnosis and seismic retrofit of existing buildings are performed nationwide in Japan. The seismic diagnosis revealed that there were many buildings of low compressive strength less than 13.5 N/mm^2 , that is defined as low strength concrete and LSC stands for low strength concrete, were found. That becomes the social problem how seismic performances for the buildings were secured with seismic retrofit. It is necessary to retrofit for the buildings of LSC so that no administration has financial surplus energy to rebuild the school buildings of LSC in the situation tight economically. Furthermore the current seismic diagnosis and retrofit standards have no application in the buildings of LSC and it is essentially to confirm the seismic performance by experiments (The Japan Building Disaster Prevention Association, 2001). However, each the evaluation organization racks its brains about the correspondence because there are few studies about LSC. Seismic diagnosis method and the seismic reinforcement technique for LSC are demanded socially by such present conditions.

The Special Research Committee on the Low Strength Concrete was organized to solve above problems, and experimental studies have been made on LSC material and members (Japan Concrete Institute, 2013). We experimented 36 columns with LSC in the committee and made a statement on some results (NEGUCHI and MINAMI, 2008).

¹ Dr. Eng., Teacher, Kochi Technical High School, Kochi, neguchi@d3.dion.ne.jp

² Dr. Eng., Visiting Professor, Chiba University, Chiba, h.tsuka@chiba-u.jp

³ Dr. Eng., Emeritus Professor, Fukuyama University, Hiroshima, minami@fucc.fukuyama-u.ac.jp

This paper reports on 2 experimental studies, the first study is the fundamental performance of test pieces with LSC retrofitted by carbon fiber reinforced plastic (CFRP), and the second study is the seismic performance of 14 experimented columns with LSC and the possibility and the effects of retrofit of columns with LSC by CFRP, furthermore an evaluation method of shear strength of columns is proposed by the plastic theory.

2. CONFINED EFFECT AND SIZE EFFECT

The first study is the experiments of the confined effect and the size effect of test pieces with LSC retrofitted by CFRP shown in Photo 1. Table 1 shows the outline of tests consisted of 8 series in 3 groups.

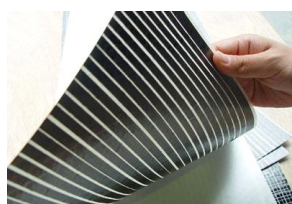


Photo 1. Carbon Fiber Sheet (CF Sheet)
















Table 1. Outline and Result of Tests

Group	Series	Shape of Section and Size	Layer of CF Sheet	$P_{w(CF)}$ [%]	Amount of Reinforcement $P_{w(CF)} \cdot \sigma_{w(CF)}$ [N/mm ²]	Compressive Strength σ_B [N/mm ²]
A	I	Round Section 100φ×200	0	0.00	0.00	9.72 (σ_{B01})
			0.5	0.11	1.79	20.93
			2.0	0.44	7.15	48.65
B	II	Round Section 100φ×200	0	0.00	0.00	8.81 (σ_{B02})
			0.5	0.11	1.79	20.18
			1.0	0.22	3.57	30.19
			2.0	0.44	7.15	49.38
	III	Round Section 150φ×300	0	0.00	0.00	8.01
			0.5	0.07	1.19	16.04
			1.0	0.15	2.38	25.66
			2.0	0.30	4.77	38.53
	IV	Round Section 150×150×300	0	0.00	0.00	7.47
			0.5	0.07	1.19	11.82
			1.0	0.15	2.38	14.87
			2.0	0.30	4.77	18.14
C	V	Round Section 100φ×200	0	0.00	0.00	13.36 (σ_{B03})
			1.0	0.22	3.57	33.32
			2.0	0.44	7.15	41.24
			3.0	0.67	10.72	60.88
	VI	Round Section 150φ×300	0	0.00	0.00	13.69
			1.0	0.15	2.38	29.32
			2.0	0.30	4.77	46.31
			3.0	0.44	7.15	32.52
			4.0	0.59	9.53	38.08
	VII	Square Section 150×150×300	0	0.00	0.00	13.37
			1.0	0.15	2.38	17.55
			2.0	0.30	4.77	22.38
			3.0	0.44	7.15	32.70
	VIII	Square Section 300×300×600	0	0.00	0.00	10.85
			2.0	0.15	2.38	13.16
			4.0	0.30	4.77	16.28
			6.0	0.44	7.15	18.81


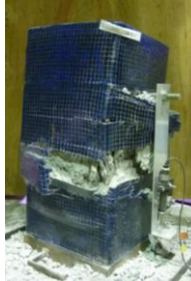


Test parameters are shape of section, size of test pieces, layers of CF sheet and compressive strength of LSC of normal non-reinforced test piece. Test pieces were casted LSC of 10N/mm^2 grade.

Test results are shown in the row of the right-side end of table 1. Photo 2 shows some cases of the failure situation. The horizontal axis represents area of section, the vertical axis represents ratio of σ_B for σ_{B0} shown in Fig. 1. σ_{B0} is the basic compressive strength of normal test piece, σ_{B1} , σ_{B2} and σ_{B3} , each group. Regardless of shape of section and size, the more compressive strength increases, the more quantity of reinforcement by CFRP increases. Compare the value of $150\phi \times 300$ with the value of $150 \times 150 \times 300$, this has about the same area of section, the effect of CFRP for round sectional test pieces are higher than square sectional ones.

The compressive strength of $300 \times 300 \times 600$ test piece is 0.73 times as the compressive strength of $100\phi \times 200$ test piece. Compared with the results of round section, the confined effect of CFRP on inside concrete of $100\phi \times 200$ test piece becomes as same as $150\phi \times 300$ test piece. Compared with the results of square section, the compressive strength of $300 \times 300 \times 600$ becomes $1/3.5$ - $1/2$ as strong as $150 \times 150 \times 300$, and it is found the effect of reinforcement by CFRP becomes relatively small as the cross section area is large. This characteristic is known a size effect. Compared with round section and square section, the confined effect on the square section becomes $1/3$ as large as round section.

Series	Shape of Section and Size	Layer of CF Sheet				
		0 (none)	1.0	2.0	3.0	4.0
V	Round Section $100\phi \times 200$					
VI	Round Section $150\phi \times 300$					
VII	Square Section $150 \times 150 \times 300$					

(a) Series V - VII

Series	Shape of Section and Size	Layer of CF Sheet			
		0 (none)	2.0	4.0	6.0
VIII	Square Section $300 \times 300 \times 600$				

(b) Series VIII

Photo 2. Examples of Failure Mode at Ultimate Compressive Strength

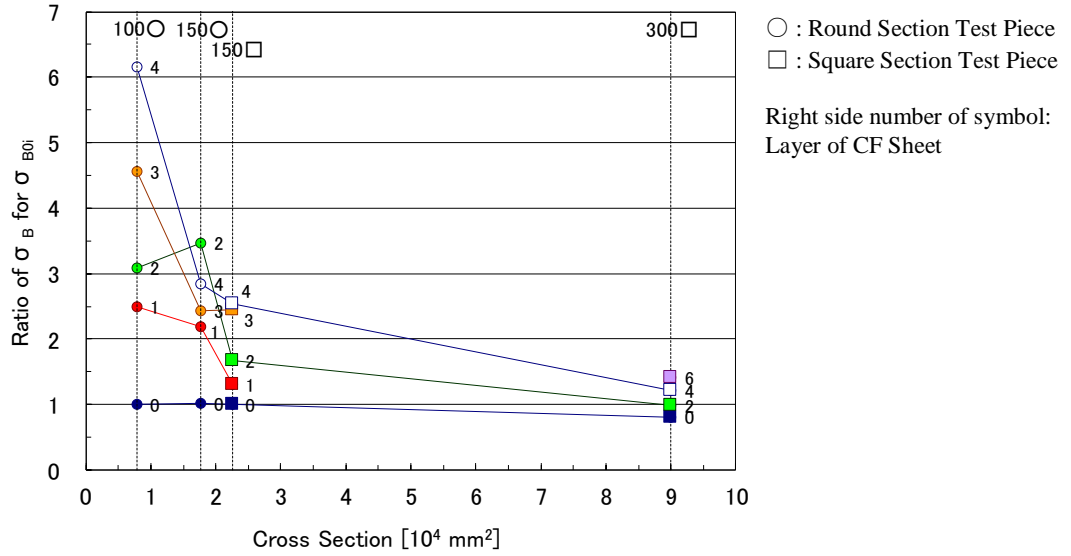


Figure 1. Relationship between Cross Section and Ratio of σ_B for σ_{B0i}

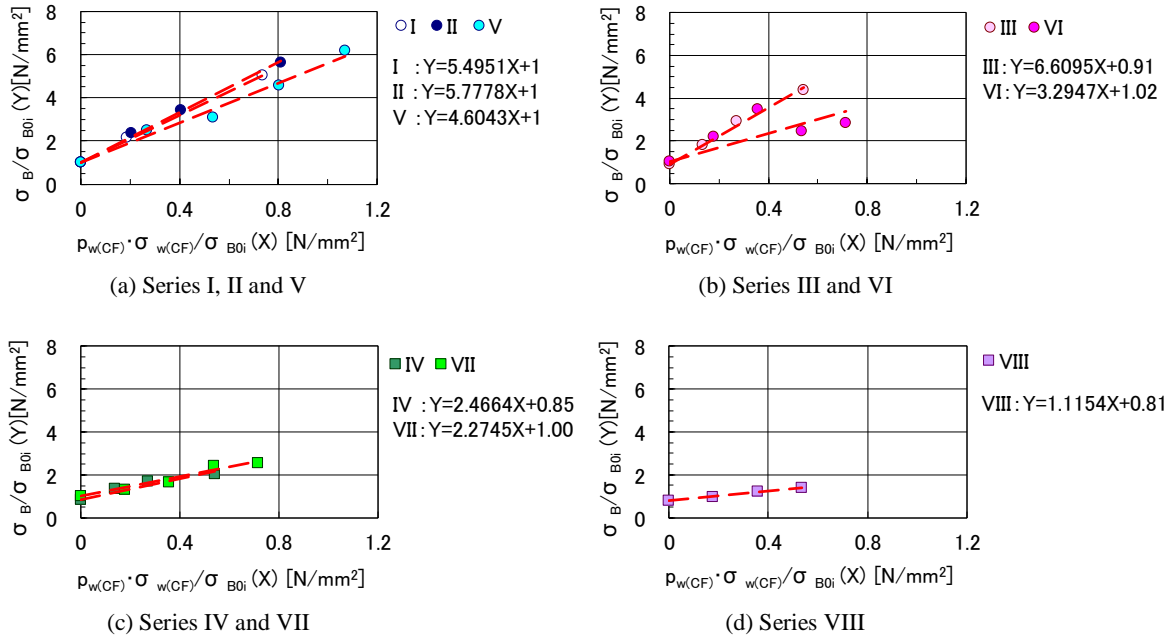


Figure 2. Relationship between Nondimensional Amount of Reinforcement and Nondimensional Compressive Strength

Table 2. Value of σ_{B0i} , A and B in Eq. (1)

Shape of Section	Size	Series	σ_{B0i}	A	B
Round Section	100p×200	I	9.72 (σ_{B01})	1.00	5.50
		II	8.81 (σ_{B02})	1.00	5.78
		V	13.36 (σ_{B03})	1.00	4.60
Round Section	150p×300	III	8.81 (σ_{B02})	0.91	6.61
		VI	13.36 (σ_{B03})	1.02	3.29
Square Section	150×150×300	IV	8.81 (σ_{B02})	0.85	2.47
		VII	13.36 (σ_{B03})	1.00	2.27
Square Section	300×300×600	VIII	13.36 (σ_{B03})	0.81	1.12

The X-axis represents $p_{w(CF)} \cdot \sigma_{wy(CF)} / \sigma_{B0i}$, and the Y-axis represents σ_B / σ_{B0i} in Fig. 2, their values are in a linear relation with the following Eq. (1). The Y value in Eq. (1) is the value of the confined effect on inside concrete.

$$Y = A + B \cdot X \quad (1)$$

where, A and B are shown in Table 3.

Compared with round section shown in Fig. 2 (a) and (b), the slope of square section is gentle shown in Fig. 2 (c), further the slope of square section and larger area is gentler shown in Fig. 2 (d). These tendency tell that the effective of reinforcement by CFRP

Meanwhile, the equation of the confined effect on inside concrete is represented in the following Eq. (2).

$$\sigma'_B = \lambda \cdot \sigma_B \quad (2)$$

$$\text{where, } \lambda = 1 + 4.1 \frac{p_w \cdot \sigma_{wy}}{\sigma_B} : \text{round section} \quad (3)$$

$$\lambda = 1 + 2.05 \frac{p_w \cdot \sigma_{wy}}{\sigma_B} : \text{square section} \quad (4)$$

p_w : shear reinforcement ratio

σ_{wy} : yield strength of shear reinforcement

σ_B : compressive strength of concrete

Eq. (2) is widely known as the equation, and λ in Eq. (3) represents the coefficient of the confined effect on round section (Richart, 1929). Chan (1955) suggested the coefficient of the confined effect on square section is half value of round section in Eq. (4). Although these equations represent the confined effect of the shear reinforcement on inside concrete, assuming that the confined effect of CFRP on inside concrete, this λ value represents the following Eq. (5) and (6).

$$\lambda = 1 + 4.1 \frac{p_{w(CF)} \cdot \sigma_{wy(CF)}}{\sigma_B} : \text{round section} \quad (5)$$

$$\lambda = 1 + 2.05 \frac{p_{w(CF)} \cdot \sigma_{wy(CF)}}{\sigma_B} : \text{square section} \quad (6)$$

where, $p_{w(CF)}$: reinforcement ratio of CF sheet

$\sigma_{wy(CF)}$: yield strength of CF sheet

σ_B : compressive strength of concrete

Although the λ value in Eq. (5) and (6) corresponds to Y value in Eq. (1), in the case of larger area of section, the λ value in Eq. (5) and (6) overestimate the confined effect. In spite of the shape of section, the larger size of section, the less the confined effect becomes. Therefore the

3. SEISMIC PERFORMANCE OF COLUMNS WITH LSC

3.1 Outline of Tests

The second study is the possibility of retrofit for columns with LSC and the effect of reinforcement by CFRP. Table 3 shows the outline of tests consisted 4 series.

Test valuables are compressive strength of concrete, 5 and 10 N/mm² grade, axial force ratio, tension reinforcement ratio and layer of carbon fiber sheet (CF sheet), shown as Table 1. 4 of 10 test specimens were non-reinforced by CFRP and the others 6 test specimens were reinforced by CFRP. The shear reinforcements in all test specimens were arranged with 2-D6 and 100mm of each shear

reinforcements interval in Table 3, and shear reinforcement ratio was $p_w = 0.21\%$. All test specimens were planned to break by shear failure.

One of the notable characteristics on this study is that the test specimens of series III and IV were experimented under higher axial load than usual axial load. The reason why such high axial force ratio is chosen is that even though same axial force, as the compressive strength of concrete becomes lower, the axial force ratio relatively becomes higher. Other notable characteristic is test specimens of series I, III, and IV are arranged with round steel bars as main reinforcements because the existing school buildings before 1965 were built with round steel bars as main reinforcements.

The loading rule experimented on by 0.2×10^{-2} rad. by the same displacement amplitude to 3.2×10^{-2} rad. twice. The axial force on test specimens was worked before working the horizontal load. Test specimens were always worked constant axial force while testing.

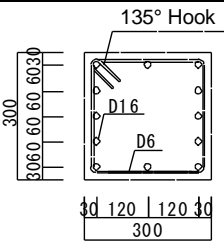
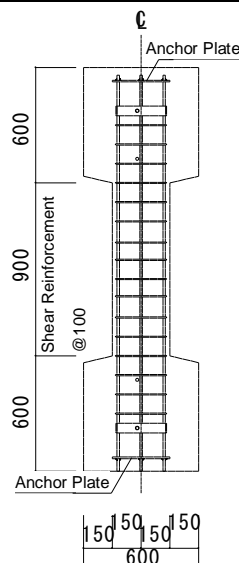
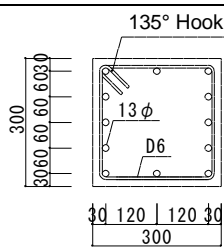
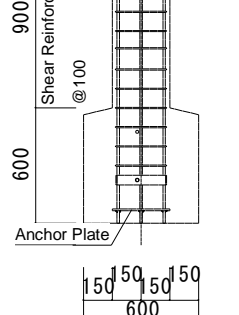
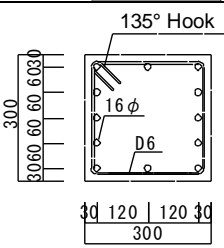
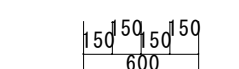
Table 4 presents the mix proportion of LSC, stress-strain curves of concrete appears in Figure 3. The notable feature of LSC is it has very ductile. Table 5 shows the characteristics of main reinforcement ($\phi 13$ and $\phi 16$) and shear reinforcement (D6). Figure 3 appears the stress-strain curves of main and shear reinforcement and CF sheet.

3.2 TEST RESULTS

The hysteresis curves are illustrated in Fig. 4 and 5, the dashed lines on curves show the calculated overturning moment value.

The hysteresis curves of columns with LSC tend to show more ductile behavior than columns with normal strength concrete, regardless of experimental variables. To put it more concretely, a few characteristics are shown on kind of main reinforcements, differences of layers of CF sheet or axial force ratio.

Table 3. Outline of Tests

Series	No.	Name of Specimens	σ_B [N/mm ²]	n	Layer of CF Sheet	p_t [%]	Cross Section [mm]	Vertical Section [mm]
I	8	L10240	13.50	0.4	none	1.12		
	13	L1024C1	9.55		0.5			
	14	L1024C2	9.60		2			
II	12	DL10240	13.89		none	1.11		
	15	DL1024C1	9.67		0.5			
	16	DL1024C2	9.74		2			
III	30	L05280S	4.69	0.8	none	0.74		
	33	L0528C2S	4.62		2			
IV	32	L10280S	10.56		none			
	34	L1028C2S	10.56		2			

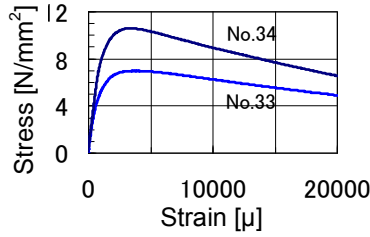
σ_B ; Compressive Strength of Concrete, n; Axial Force Ratio $n = N/(b \cdot D \cdot \sigma_B)$, N; Axial Force [N], , CF Sheet; 200 [g/m²]

Table 4. Mix Proportion of Low Strength Concrete

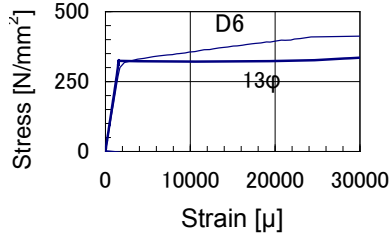
Specified Design Strength [N/mm ²]	5	10
Water [kg/m ³]	210	210
Sand Percentage [%]	49.9	50.2
Water/Binder Ratio [%]	65.0	65.0
Water/Cement Ratio [%]	221.0	122.0

Table 5. Tensile Test Result of Steel Reinforcement

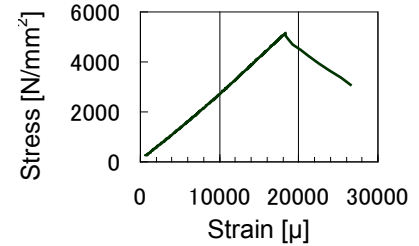
Steel	Yield Strength [N/mm ²]	Young's Modulus [N/mm ²]
16φ	340	1.88×10 ⁵
D16	372	1.77×10 ⁵
13φ	320	2.01×10 ⁵
D6	320	1.92×10 ⁵



(a) Concrete



(b) Reinforcement



(c) Carbon Fiber Sheet

(by Nippon Steel Composite Co., Ltd.)

Figure 3. Stress-Strain Curves of Materials

Compared hysteresis curves of the series I and II, the strength of series II column with deformed bars as main reinforcements suddenly decreases after maximum strength. On the other hand, the strength of columns with round bars as main reinforcements pretty gently or hardly decreases. Though the tendency after the maximum strength is shown regardless of reinforced or non-reinforced test specimens, it is clearer on non-reinforced test specimens. The hysteresis curves show that the strength of columns with round bars as main reinforcement hardly decreasing even on non-reinforced column. Such tendency shows the stronger on the column reinforced with the more layers within two layers of CFRP.

It is characteristic for the columns tested under high axial load of the series III and IV to be reinforced by CFRP, especially for the column with high axial force ratio and deformed bars as main reinforcements. This seismic reinforcement theory is effective for even LSC columns.

4. EVALUATION METHOD OF SHEAR STRENGTH BY PLASTIC THEORY

The evaluation of the ultimate shear strength of LSC columns calculates by the plastic theory which allows the mixed model of the truss mechanism and the arch mechanism as the shear resistance mechanism.

The nondimensional shear strength of the truss mechanism is calculated by the minimum value between the tensile strength of mainreinforcement, the bond strength on main reinforcement and the yield strength of shear reinforcement as illustrated in Fig. 6. The truss mechanism is consisted of main reinforcement to resist tensile or compressive force and the concrete strut. The concrete strut makes an angle ϕ with the longitudinal main reinforcement, and the width of the concrete strut is b_t as illustrated in Fig. 6.

Assuming that the angle of inclination of the unyield shear reinforcement is $\phi=45^\circ$ for transmitting the bond strength, the concrete compressive strength σ_B is kept in the concrete compressive field in Fig. 7. The nondimensional truss strength q_{Ut} is evaluated by Eq. (7).

$$Q_{Ut} = \tau_{Ub} \cdot \Sigma \phi \cdot D \quad (7)$$

$$\text{where, } \tau_{Ub} = \frac{\varepsilon \cdot A \cdot E}{\ell \cdot \phi} \quad (8)$$

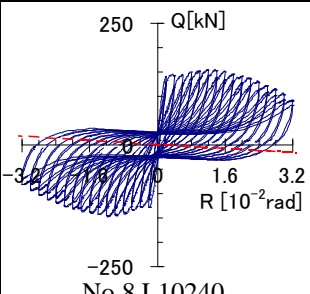

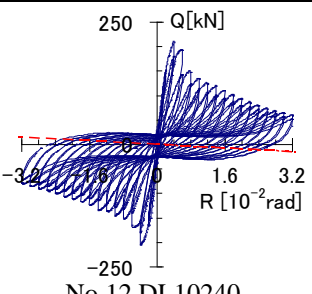

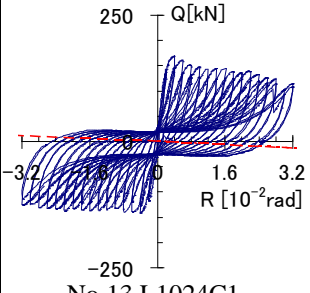

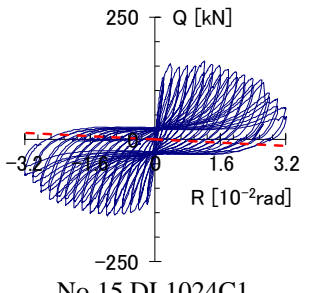

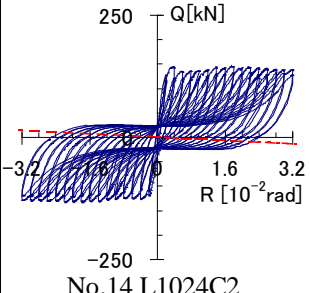

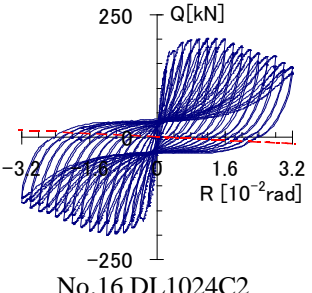

Series	I	II
Main Reinforcement	Round Bar ($\phi 16$)	Deformed Bar (D16)
None of CF Sheet (Non-Retrofit by CFRP)	  <p>No.8 L10240</p>	  <p>No.12 DL10240</p>
0.5 Layer of CF Sheet	  <p>No.13 L1024C1</p>	  <p>No.15 DL1024C1</p>
2 Layers of CF Sheet	  <p>No.14 L1024C2</p>	  <p>No.16 DL1024C2</p>

Figure 4. Hysteresis Curves and Failure Mode at Ultimate Strength

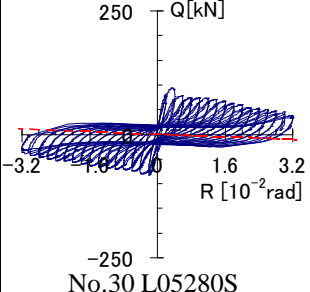

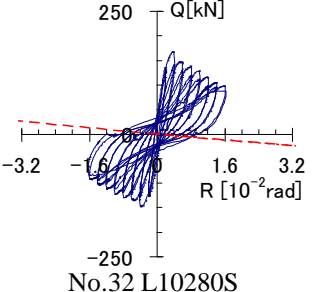

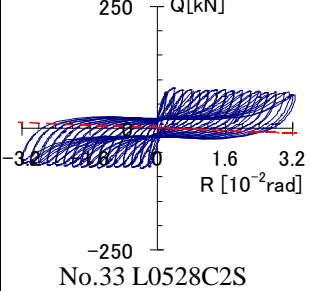

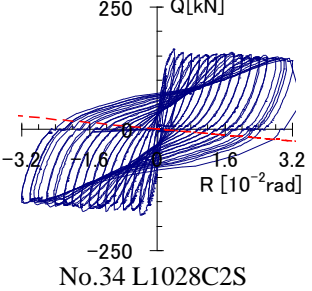

Series	III	IV
None of CF Sheet (Non-Retrofit by CFRP)	  <p>No.30 L05280S</p>	  <p>No.32 L10280S</p>
2 Layers of CF Sheet	  <p>No.33 L0528C2S</p>	  <p>No.34 L1028C2S</p>

Figure 5. Hysteresis Curves and Failure Mode at Ultimate Strength

ε : strain of main reinforcement, A : area of main reinforcement [mm^2],
 E : Young's modulus [N/mm^2], ℓ : bond splitting length [mm],
 φ : perimeter of longitudinal reinforcement [mm]

in addition, for establishing the mechanism, the width b_t of concrete compressive field is given by Eq. (9).

$$b_t = 2 \cdot \frac{\tau_{Ub}}{\sigma_B} \cdot \Sigma \varphi \quad (9)$$

It is assumed that the arch mechanism as illustrated in Fig. 7 is constituted when the resultant uniaxial compressive stress, σ_o , of the normal stress, σ_p , both uniformly distributed over the compression region at both ends of the reinforcement-less concrete with the width b_a , which is the remaining width used for the arch mechanism and given by Eq. (10), are produced in the direction that is off from the member axis by the angle of θ . Further, the maximum shear resistance of the arch mechanism is assumed to take place when the above-mentioned resultant stress, σ_o , reaches σ_B , when the shear strength, Q_{Ua1} , can be expressed by Eq. (11).

$$b_a = b - b_t \quad (10)$$

$$Q_{Ua1} = \left[\sqrt{4 + \left(\frac{\eta}{c n_0} \right)^2} - 4 c n_0^2 - \left(\frac{\eta}{c n_0} \right) \right] \cdot \frac{b_a \cdot D \cdot \sigma_B}{2} \quad (11)$$

$$\text{where, } \eta = h/D \quad (12)$$

$$c n_0 = \sqrt{\frac{\sqrt[3]{\eta^2 + \eta^2 \sqrt{1 + \eta^2}}}{2} + \frac{\sqrt[3]{\eta^2 - \eta^2 \sqrt{1 + \eta^2}}}{2}} \quad (13)$$

The Q_{sU2} is given by superposition of Q_{Ut} and Q_{Ua1} by Eq. (14).

$$Q_{sU2} = Q_{Ut} + Q_{Ua1} \quad (14)$$

Furthermore, the confined effect for concrete is evaluated by Eq. (15). Chan (1955) suggests 2.05 as the coefficient of column with square cross section in Eq. (16), this coefficient is half of the coefficient for circular cross section by the research of Richart (1929). The result of our experiment shows that it is reasonable to apply these coefficients to LSC.

$$\sigma'_B = \lambda \cdot \sigma_B \quad (15)$$

$$\text{where, } \lambda = 1 + 2.05 \frac{P_w \cdot \sigma_{wy}}{\sigma_B} \quad (16)$$

Let σ'_B be σ_B in Eq. (11), the strength of the arch mechanism considered the confined effective for concrete is given by Eq. (17).

$$Q_{Ua2} = \lambda \cdot Q_{Ua1} \quad (17)$$

Then, the ultimate shear strength Q_{sU3} is given by superposition Q_{Ut} and Q_{Ua2} by Eq. (18).

$$Q_{sU3} = Q_{Ut} + Q_{Ua2} \quad (18)$$

Fig. 9 illustrates the relationship between calculate shear strengthb by Eq.(18) and experimental shear strength. The continuous line in figure is an approximately straight line, and shows calculated ultimate shear strength by Eq. (18) agrees the experimental results.

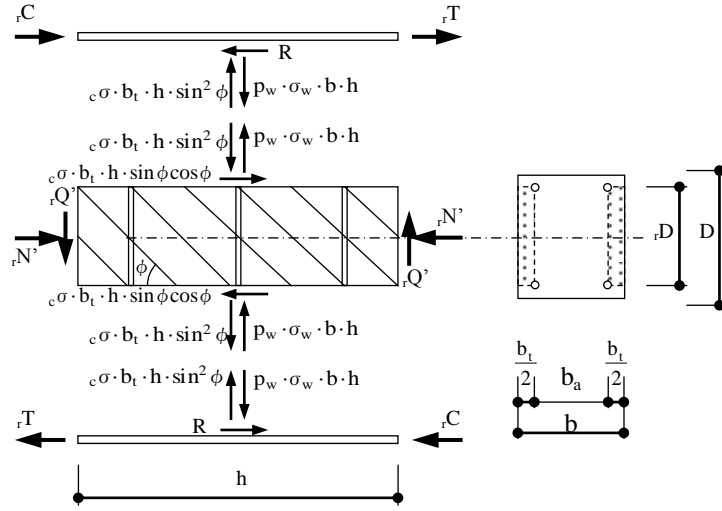


Figure 6. Truss Mechanism

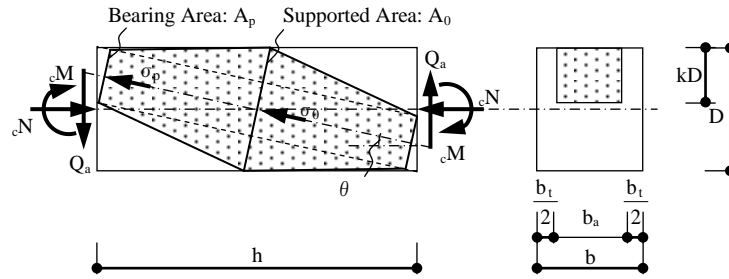


Figure 7. Arch Mechanism

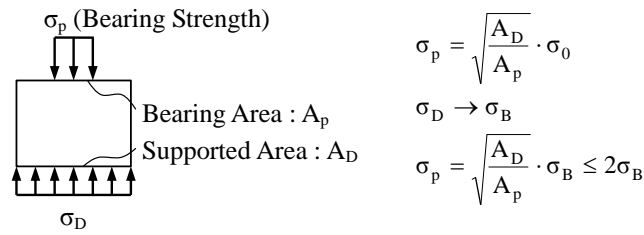


Figure 8. Bearing Strength

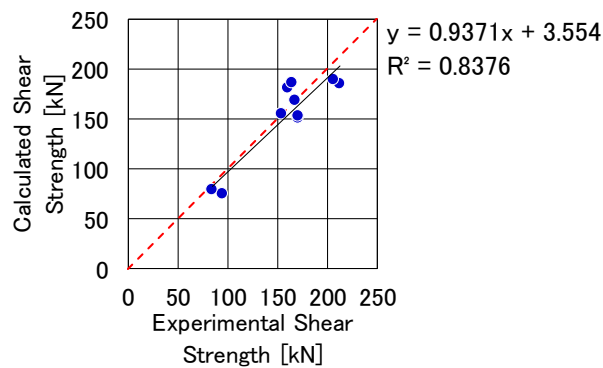


Figure 9. Relationship between Calculate Shear strength and Experimental Shear Strength

5. CONCLUSIONS

The following results were obtained in this paper:

- (1) Even if the column with LSC of 5 N/mm^2 grade and round bars as main reinforcements, it was able to perform cyclic load to the displacement amplitude of 3.2×10^{-2} rad., did not finally occur the decreased strength.
- (2) The confined effect of CFRP on inside concrete of large square column is uncalculated.
- (3) The ultimate shear strength is able to evaluate by the plastic theory.
- (4) Even columns with LSC have the performance as columns and can be retrofitted by CFRP.

REFERENCES

- Architectural Institute of Japan (1990). Design Guideline for Earthquake Resistant Reinforced Concrete Buildings Based on Ultimate Strength Concept, (in Japanese)
- Chan, W. W. L. (1955) "The Ultimate Strength and Deformation of Plastic Hinges in Reinforced Concrete Frameworks", *Magazine of Concrete Research*, Vol. 7, No. 21, 121 -132
- Japan Concrete Institute (2013), The Research Report on Special Research Committee on the Low Strength Concrete, (in Japanese)
- NEGUCHI, Momoyo and MINAMI, Koichi (2008) "Some Considerations on Strength and Ductility of RC Members with Low Strength Concrete", *14th World Conference on Earthquake Engineering*, 05-03- 0236, Beijing, China, 8 pages
- Neguchi, M. and Minami, K. (2009) "Some Considerations on Strength and Ductility of RC Members with Low Strength Concrete", *Proceeding of the 2009 ANCER Workshop*, University of Illinois, 8 pages, Urbana, Illinois, United States
- NEGUCHI, Momoyo and MINAMI, Koichi (2010) "Seismic Evaluation of Low Strength Concrete Members of Existing Buildings in Japan" , *14th European Conference On Earthquake Engineering*, 782, 8 pages, Ohrid, Republic of Macedonia
- The Japan Building Disaster Prevention Association (2001) Seismic Evaluation Standard for Existing Reinforced Concrete Structure, Japan, (in Japanese)
- Richart, F. E., Brandtzaeg, A. and Brown, R. L. (1929) "The Failure of Plain and Spirally Reinforced Concrete in Compression", *Engineering Experiment Station*, Bulletin No. 190, University of Illinois